

Drag Reduction In Turbulent Flow using Different Kinds of Riblets

Imad S. Ali
Asst. Professor
University of Babylon
Hilla- Iraq
Emad.ali6@gmail.com

Noor H. Al-Fatlawie
M. Sc University of Babylon
Hilla- Iraq
Noor_h1987@yahoo.com

Abstract— In the present work the characteristics of a turbulent flow field over a riblet surface plate models have been investigated experimentally and compared with a smooth surface. Experiments tests were carried out in a low speed open-typed wind tunnel at constant air speed 20m/s and Reynolds number 4.9×10^5 based on length of plate. Drag reduction investigations in a turbulent flow over a riblet-covered surface is performed for two models: straight riblets and sinusoidal riblets with ratio ($a/\lambda=0.01$). A parametric investigations show that the riblet shape, height (h), width (w) and lateral spacing (s) are main factors affecting drag reduction. With straight riblets model, skin friction drag reduction in the range of 10–14% have been obtained, and the best dimension are (h=0.25mm, s=1mm and w=1mm). The results show that more significant drag reduction is achieved with sinusoidal riblets due to an oscillatory spanwise component added to the mean flow, and it is found that drag reduction depend strongly on the a/λ ratio. Sinusoidal riblet surface reduces drag coefficient by 19%, and the best dimensions for this riblet model to give high drag reduction are (h=0.125 & 0.25mm, s=2mm and w=2mm).

Keywords- Riblet surface; Drag reduction; Turbulent boundary layer.

I. INTRODUCTION

Several international meetings have addressed the subject of riblets, both from the view point of basic fluid mechanics as well as practical applications. Drag reduction of civil transport aircraft directly concerns performance, but also indirectly, of course, cost, and environment. Fuel consumption represents about 22% of the direct operating cost which is of utmost importance for the airlines, for a typical long range transport aircraft. Drag reduction directly impacts on the direct operating cost: a drag reduction of 1% can lead to a operating cost decrease of about 0.2% for a large transport aircraft.

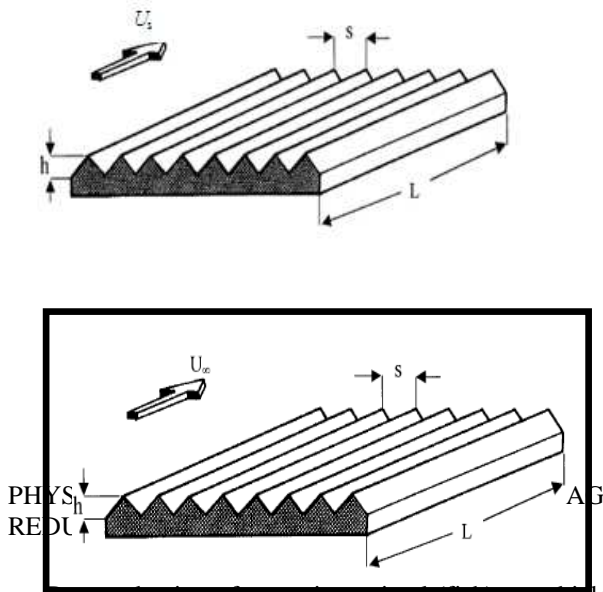
Control of turbulent flows, turbulent boundary layers in particular, has been a subject of much interest owing to the high potential benefits. Skin-friction drag constitutes a large fraction of the total drag on commercial aircrafts and cargo ships, and any reduction entails substantial savings of the operational cost as well as obvious advantages of increased speed and/or efficiency.

Although it has been common knowledge in fluid mechanics that the skin-friction drag in turbulent

boundary layers is much higher than that in laminar boundary layers, it was not until recently that we began to understand why this was the case. Since the underlying physics of high skin friction drag were not known, most attempts to reduce the drag were on a trial-and-error basis. Existence of well-organized turbulence structures and the recognition that these structures play important roles in the wall-layer dynamics are among the major advances in turbulent boundary layer research during the past several decades. Thus, further investigations of this phenomenon could prove fruitful. The ubiquitous structural features in this region are low- and high-speed “streaks,” which consist mostly of a spanwise modulation of the streamwise velocity. These streaks are created by streamwise vortices, which are roughly aligned in the streamwise direction. It has now been recognized that streamwise vortices are also responsible for the high skin friction drag [9]. These vortices are primarily found in the buffer layer ($y^+ = 10 - 50$) with their typical diameter in the order of ($d^+ = 20 - 50$) [4].

Due to the restriction of the wall, the fluid particles near wall, under the active of the viscous stress and the turbulent stress, not only undergo a pulsation along the flow direction, but also undergo a transversal turbulent diffusion. The boundary layer along the normal distance of the wall can be divided into two regions: wall and core filed. The former can be further divided into viscous bottom, transition layer and logarithmic rule layer. The field between viscous bottom and transition layer is called near wall region, whose thickness approximately equals twenty percents of the thickness of the boundary layer. The formation and development of turbulence mainly appear in this region. Therefore, it is reasonable to analyze the mechanism of the drag reduction over riblet surfaces through the characteristic of the flow in the near – wall, fig. 1.

The most important characteristics of the turbulent structure in the near wall region is the burst phenomenon [4]. The burst comprises five stages: the low speed fluid ejected from the wall region, the rising of low speed fluid, vibration, burst and sweeping. The burst consumes the energy of the flow over the walls. The basic idea of turbulent boundary drag reduction is to avoid the streamwise concentration of low – speed streak, to restrain turbulent bursting and to reduce turbulent dynamic energy.



Drag reduction of a moving animal (fish) or vehicle can be achieved by reducing wall shear stress. By about a decade ago it had become clear that a turbulent boundary layer on a surface with longitudinal ribs can develop a lower shear stress than that on a smooth surface. For a possible mechanism of turbulent drag reduction with riblets, several concepts have been proposed. Reference [3] considered the interaction of the counter-rotating longitudinal vortices with the small eddies created by them near the peaks of riblets, arguing that the secondary vortices would act to weaken the longitudinal vortices, which bringing high-speed fluid towards the wall during the turbulent sweep events, as well as to retain the low-speed fluid within the grooves. They conjectured that the secondary vortices at the riblet tips weaken the streamwise vortices, developing near the surface beneath a turbulent boundary layer, and inhibit the spanwise movement of streaks, necessary to replace the near wall fluid that is ejected during turbulence production events, thereby restricting momentum exchange in the lateral direction caused by the streamwise vortices. In other words, The streamwise vortices are displaced away from the wall, and the turbulent mixing of streamwise momentum is reduced. Since this mixing is responsible for the high local shear near the wall [10], its reduction results in a lower skin friction.

Reference [6] found that the sharp ridges of the riblets impede cross-flow induced by the overlying streamwise vortices in the viscous sublayer and that the presence of the rebllits decrease turbulent inetensity momentum exchange in the boundary layer, reducing turbulent energy and shear stress. In this layer, very close to the wall, any fluid behaves like a highly viscous fluid. Therefore it is admissible to calculate the flow around very small ribs with a viscous theory.

The riblets work like small fences restricting the lateral movement or meandering of the longitudinal vortices Fig. 2, less low – speed streak wavering and flow within riblets is slow and quiescent, this reduces the intensity of the downwash during the near wall burst, which constitutes a large part of turbulent skin friction.

Drag reduction by riblike surfaces makes sense only where turbulent wall friction makes an important contribution to fluid-dynamic losses. However, in other cases, such as in automobile aerodynamics, which is governed by separated flow and form drag, the application of riblet film would be useless [12].

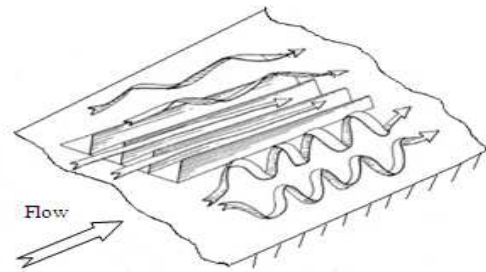


Figure 2. Riblet drag reduction (taken from [5]).

III. EXPERIMENTAL WORK

The experiments performed in an open circuit type, low speed wind tunnel. The objective of the experimental investigation carried out in the present work is to determine the effect of (longitudinal and sinusoidal) riblets on the development of the boundary layer and flow characteristics over the test surfaces. The wind tunnel used in all these experiments is capable of continuous airspeeds up to 30m/s, operating on working fluid (air), Fig. 3. This wind tunnel is the simplest and most affordable to build. The testes were performed at a freestream velocity of $U_s=20\text{m/s}$ Providing Reynolds number, $Re = 4.9 \times 10^5$ based on length of plate.



Figure 3. Photo for wind tunnel.

Velocity and pressure distribution close to the upper surface of the plate measurements using a pitot-static tube connected to multi tube manometer. Three interchangeable plates $b=150\text{mm}$ wide, $L=400\text{mm}$ long and 2mm thick were machine cut from soft steel and available for the experiment, one with a smooth surface and the other two with a riblet surfaces. The leading edge of the plate was 85mm downstream from the beginning of the measuring test section of the wind tunnel. A cylindrical trip-wire 0.9mm in diameter was used and positioned 10mm downstream from the leading edge [13], for each model to make a fully

developed turbulent boundary layer at the measurement location.

Conventional, or two-dimensional riblet with rectangular cross-section has been chosen aligned in the direction of the freestream flow, Fig. 4. The modified riblet geometry is obtained from a conventional geometry by changing the shape of the riblets in spanwise direction from straight line to sinusoidal waves as demonstrated in Fig. 5, and become three-dimensional, rather than two-dimensional structures. The riblets were installed at 115mm downstream from the leading edge of the base plate. Sinusoidal riblet were made in the same way for the straight riblet and same dimensions but the riblets are oscillating with a period of oscillation. Two more parameters are therefore introduced by changing the shape of the riblets, amplitude a and wavelength λ of the sinusoidal shape function.

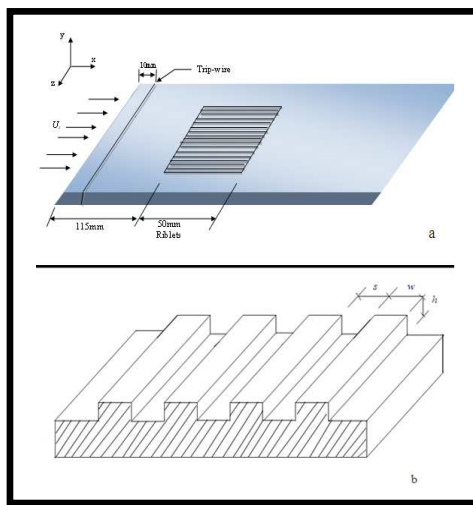


Figure 4. a- Schematic diagram of test plate. b- Cross-section view of straight riblet surface.

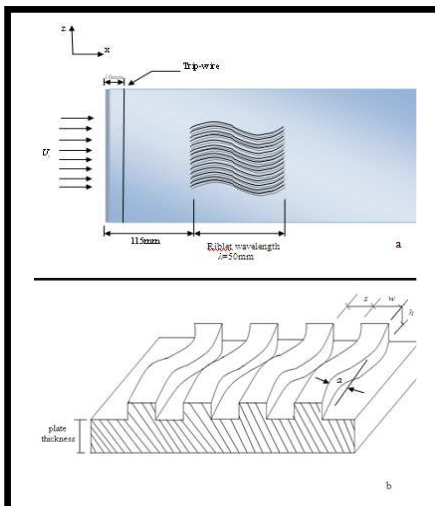


Figure 5. a- Schematic diagram of test plate. b- Cross-section view of sinusoidal riblet surface.

The turbulent flow over sinusoidal riblet-covered surface is performed for ratio $a/\lambda=0.01$. The purpose of the experiments is to study the change of parameters height (h), width (w) and riblet spacing (s) on the

percent of drag reduction to reach the optimum dimensions of h , s and w that the best drag reduction for rectangular riblets. Dimensions of riblet are summarized for two models in Table 1.

In order to investigate the flow field over flat plate with smooth and different riblet surfaces, a velocity distribution along the surface is required which measured by using pitot-static tube. The momentum thickness of boundary layer was determined using:

$$\theta = \int_0^\delta \frac{u}{U_s} \left(1 - \frac{u}{U_s}\right) dy \quad (1)$$

δ is the boundary layer thickness. The momentum thickness distribution on the flat and riblet surfaces can be used to calculate the friction drag [1], using:

$$D(x) = b\rho U_s^2 \theta(x) \quad (2)$$

Here $D(x)$ denotes the friction drag at a distance x from the leading edge.

The wall shear stress is defined as:

$$\tau(x) = \rho U_s^2 \frac{d\theta}{dx} \quad (3)$$

Moreover, using the shear stress equation, the values of the skin friction coefficient can be determined by non-dimensionalizing the wall shear stress in eq. (4), where,

$$C_f = \frac{\tau}{\frac{1}{2} \rho U_s^2} \quad (4)$$

The turbulent drag reduction, R_D , was computed as the percent difference in skin friction coefficient at the riblet and no-riblet surface [16] by the following equation:

$$R_D = \frac{C_{f \text{ no-riblet}} - C_{f \text{ riblet}}}{C_{f \text{ no-riblet}}} \quad (5)$$

IV. RESULTS AND DISCUSSION

Experiments were carried out using two different riblet models (longitudinal and sinusoidal) are compared to the smooth flat plate surface. The tests have been achieved for turbulent, incompressible, viscous, steady flow and two dimensional.

A. Mean velocity profiles

Fig. (6 - 8) show the mean velocity profiles for straight and sinusoidal riblet models. For most riblet cases in the present investigation, the velocity profiles shift slightly downward compared with the smooth surface, it is clear that the wall normal mean velocity gradient is lower for cases of drag reduction, which happens for two reasons: the decrease in the friction velocity u_τ ($u_\tau^2 = \tau/\rho$), and the reduction in the vorticity of the fluid, Both effects shift the profiles in this direction.

B. Riblet effect on the momentum thickness

The momentum thickness distribution calculated for the 2D straight riblet model shown in Fig. (9 and 10a) and for 3D sinusoidal riblet model shown in Fig. (10b and 11) compared with the smooth plate surface. Each figure include riblet cases with two common dimensions. Riblet surface reduce the momentum thicknesses in a boundary layer compared to the flat surface due to lower wall normal mean velocity

gradient near the wall. However, the results presented here demonstrate that large flow modification can be obtained with boundary layer riblet geometry.

C. Skin friction coefficient

• Straight model results:

The coefficient of friction for all straight riblet cases tracks with that of the smooth surface, as in Fig. (12 and 13a), the results show that C_f at the riblet surface for most of the cases is smaller than the C_f at the flat surface. In the present experiments, maximum drag reduction of approximately 14% was observed for riblet cases (case. 2 and 5) as shown in table 1, this is in fact close to the experimental results obtained by [2] (where reduction is of 16%) and main conclusion of the numerical work of [16] (where reduction is of 13%) for the same configuration. The coefficient of friction of the riblet surfaces were found to lie well below those of the smooth surface; this is due to the riblets restrain the cross – flow motion of the streamwise vortices which are associated with creation of high skin friction zones in a turbulent boundary layer. Riblet cases (case. 6 and 9) show a somewhat smaller drag reduction than that which are noted by cases above. This results is likely due to differences in the riblet dimensions. drag reduction is reduced to a negative value for the riblet cases (case. 4 and 7), as shown in table 1, this due to the friction and drag increasing on the riblet surface.

• Sinusoidal model results:

Fig. (13b and 14) show the resulting skin friction coefficient calculations for the smooth and sinusoidal riblet surfaces with ($a/\lambda=0.01$). There is significant decrease in C_f for riblet (case.5), this corresponds to 19% drag reduction, which is almost 27% larger than the drag reduction observed with the straight riblet model, the drag reduction were dependent on the geometry and dimensions of riblet alone. The reduction in drag are associated with the significant reduced in cross flow turbulence which enhance the skin friction drag. This consistent with suppression streamwise vortices. When transverse turbulent fluctuations are reduced, turbulent momentum transfer close to the surface is also reduced, and, consequently the skin friction is decreased [11].

D. Wall shear stress

Fig. (15 - 17) show the wall shear stress distribution on the plate surface with and without riblet for straight and sinusoidal models. The smooth surface has a higher wall shear stress than the riblet surface for the most cases. Wall shear stress reduction on the riblet surface cases (case. 2, 3, 5, 8 and sinus 5) have more reduction in shear stress than other cases. The shear stress reduction mechanism by riblets is as follows: the riblets impede the cross – flow motion by restraining the fluctuation cross – flow component for the streamwise vortices. This leads to the reduction in a turbulent momentum transfer close to the wall, and, consequently the turbulent shear stress is decreased [7]. The shear stress for the straight riblet surfaces (case. 4

and 7) increase, as shown in Fig. (15a and 15b) respectively.

E. Drag performance with riblet dimensions

Fig. 18 (a and b) shows the variation of the drag reduction R_D with increasing riblet height for riblet models (straight and sinusoidal), while s and w kept constant. The observation suggest that drag reduction due to riblets can be increases up to a riblet height ($h=0.25$), then decreases gradually with increasing riblet height. The drag reduction for straight riblet , Fig. 14a, increased initially with riblet height from about 5% at ($h=0.125$ mm) to 14% at ($h=0.25$ mm) then decrease to -15%, i.e increase in drag, at ($h=0.75$ mm). Also the percentage of drag reduction for sinusoidal model, Fig. 14b, increased initially with h from 8.6% at ($h=0.125$ mm) to 14% at ($h=0.25$ mm) and 4% at ($h=0.5$ mm) then decrease to 1.3% at ($h=0.75$ mm), this is because the influence of riblets on the activity of longitudinal vortices, so drag reduction takes place in such range.

This indicates that the height of the riblets is important factor in drag reduction and there was limit for increasing h because more increasing of h decreasing the effect of drag reduction and becomes drag increase. The results show that high drag reduction can be obtained with variations in geometry and dimensions of riblets. The best dimensions of the straight model with rectangular cross section which give a high reduction in drag are ($h=0.25$ mm, $s=1$ mm and $w=1$ mm), and for sinusoidal model are ($h=0.125$ and 0.25 mm, $s=2$ mm and $w=2$ mm).

F. Comparison between straight and sinusoidal models results

Comparison between the results of the skin friction coefficient for straight and sinusoidal riblet surface models is shown in Fig. 19. The riblets influence can be clearly distinguished. For comparison, the result of friction coefficient for the smooth surface is superimposed over the data in this figure. Sinusoidal riblet model reduced the C_f rather than the straight model, a maximum skin friction drag reduction of 19% for the $a/\lambda=0.01$. This indicates that the drag reduction was dependent on the geometry and riblet dimensions alone. For the sinusoidal model, however, there is a third parameter of importance, the a/λ ratio of the sinusoidal oscillation.

G. Comparison of the present work with others researches

The comparison of the mean velocity profiles for both riblet models with literature are shown in figures (20-22), the law of the wall is also given in these figures. The velocity profile for straight model is compared with the results of [15] and [16] , and with [14] for sinusoidal. All profiles show a significantly lower velocity in the lower buffer layer and an increased velocity in the logarithmic region. This increase is the direct result of the reduced skin friction.

TABLE 1. RIBLET CASES AND RESULTS OF DRAG REDUCTION

Riblet cases	Width, w (mm)	Spacing, s (mm)	Height, h (mm)	Drag Reduction R_D %
2D Straight model				
<i>(w, s) constant</i>				
Case. 1	1	1	0.125	5
Case. 2	1	1	0.25	14
Case. 3	1	1	0.5	10.3
Case. 4	1	1	0.75	-15
<i>(w, h) constant</i>				
Case. 5	2	1	0.25	14
Case. 6	2	2	0.25	2
Case. 7	2	3	0.25	-15
<i>(s, h) constant</i>				
Case. 8	1	2	0.25	13.2
Case. 6	2	2	0.25	2
Case. 9	3	2	0.25	1.5
3D Sinusoidal model				
<i>(w, s) constant</i>				
Case. 1	1	2	0.125	8.6
Case. 2	1	2	0.25	14
Case. 3	1	2	0.5	4
Case. 4	1	2	0.75	1.3
<i>(s, h) constant</i>				
Case. 1	1	2	0.125	8.6
Case. 5	2	2	0.125	19
<i>(w, h) constant</i>				
Case. 6	1	1	0.125	3.5
Case. 1	1	2	0.125	8.6

CONCLUSIONS

From the discussion of the experimental results for the present work, the following conclusions may be drawn:

- The near-wall mean velocity profile over riblet surfaces was shifted downward compared with the smooth surface which implied a decrease in the velocity gradient for the flow over the riblet surface.
- The turbulent flow properties, as well as the boundary layer characteristics, were altered by the surface modification. This indicates that there is reduce in the value of displacement and momentum thickness.
- The skin friction coefficient over riblet surface is generally less than the skin at a smooth wall.
- The reduction in the shear stress was observed for most riblet cases in the present study, indicating small skin friction with riblet surfaces.
- By introducing spanwise sinusoidal variation to the riblet shape can be an effective drag reduction method showing benefits compared to the conventional straight riblets with the correct choice of geometrical parameters.
- For straight riblet, maximum drag reduction of 14% is observed for cases 2 and 5. For sinusoidal riblets with $a/\lambda=0.01$, maximum drag reduction of 19% is observed for case.5.
- The results of drag reduction have been given as a function of the riblet parameters [height (h), width (w), and riblet spacing (s)]. The best dimensions of the straight riblet model which give a high reduction in drag are ($h=0.25$ mm, $s=1$ mm and $w=1$ mm), and for sinusoidal model are ($h=0.125$ & 0.25 mm, $s=2$ mm and $w=2$ mm).
- Results show that drag reduction is strongly depending on the geometry and dimensions of riblets. The best geometry of two models is sinusoidal model. Oscillatory tilting of riblets has the capability to improve drag reduction by about 27% compared with straight model.

REFERENCES

- [1] H. Schlichting, "Boundary layer theory", New York: McGraw-Hill, 1979.
- [2] M. J. Walsh, "Turbulent boundary layer drag reduction using riblets", AIAA paper, Vol. 82, 1982.

[3] E. V. Bacher, C. R. Smith, "Turbulent boundary layer modification by surface riblets", AIAA Journal, Vol. 24, pp.1382–1385, 1986.

[4] J. Kim, P. Moin, R. D. Moser, "Turbulence statistics in fully developed channel flow at low Reynolds number", Fluid Mech. 177, 133, 1987.

[5] M. J. Walsh, W. L. Sellers, "Riblet drag reduction at flight condition", AIAA Paper 88–2554, 1988.

[6] D. W. Bechert, M. Bartenwerfer, "The viscous flow on surfaces with longitudinal ribs", Fluid Mech. 206, pp.105–129, 1989.

[7] K. S. Choi, R. Johnson, "Near wall structure of a turbulent boundary layer with riblets", Fluid Mech. Vol. 208, pp. 417–458, 1989.

[8] J. P. Robert, "Drag reduction: an industrial challenge", special course on skin friction drag reduction, AGARD- R- 786, Paper No.2, 1992.

[9] H. C. Choi, P. Moin, J. Kim, "Direct numerical simulation of turbulent flow over riblets", Fluid Mech. Vol. 255, pp. 503–539, 1993.

[10] P. Orlandi, J. Jiménez, "On the generation of turbulent wall friction", Phys. Fluids, Vol. 6, pp. 634–641, 1994.

[11] D. W. Bechert, M. Bruse, W. Hage, T. Van der Hoeven, G. Hoppe, "Experiments on drag – reducing surfaces and their optimization with an adjustable geometry", Fluid Mech. Vol. 338, pp.59–87, 1997.

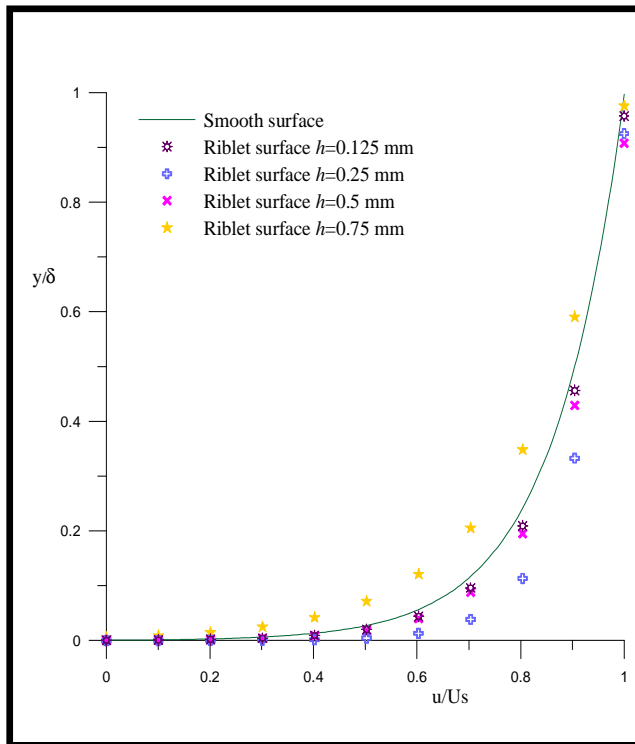
[12] D. W. Bechert, M. Bruse, W. Hage, R. Meyer, "Fluid mechanics of biological surfaces and their technological application", Springer – Verlag, Vol. 87, pp. 157–171, 2000.

[13] G. B. Brian, B. Raúl, G. Johansson, L. Castillo, "Transitionally rough zero pressure gradient turbulent boundary layers", Experiment in Fluids, Vol. 44, pp. 115–124, Springer–Verlag 2008.

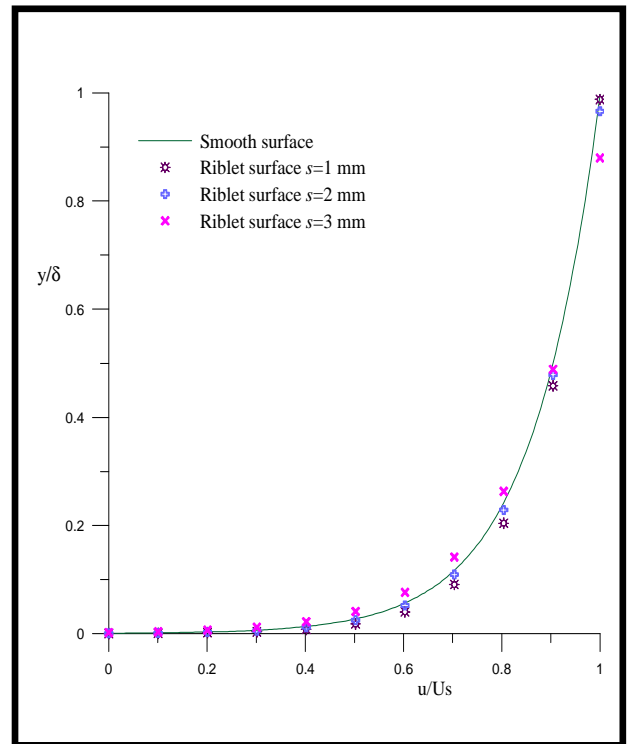
[14] Y. Peet, P. Sagaut, "Turbulent drag reduction using sinusoidal riblets with triangular cross-section", AIAA Fluid Dynamics, Vol. 38, 2008.

[15] E. Wassen, F. Kramer, F. Thiele, "Turbulent drag reduction by oscillating riblets", AIAA 4th Flow Control conference, 2008.

[16] M. E. Benhamza, F. Belaid, "Computation of turbulent channel flow with variable spacing riblets", MECHANICA. Vol. 79, pp. 1392–1207, 2009.

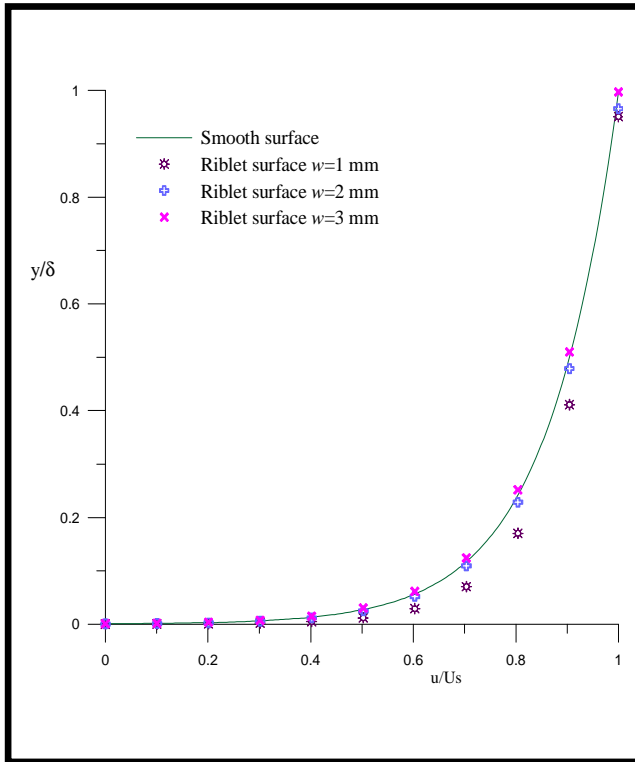


(a) Straight riblet with $w(=s)=1\text{mm}$

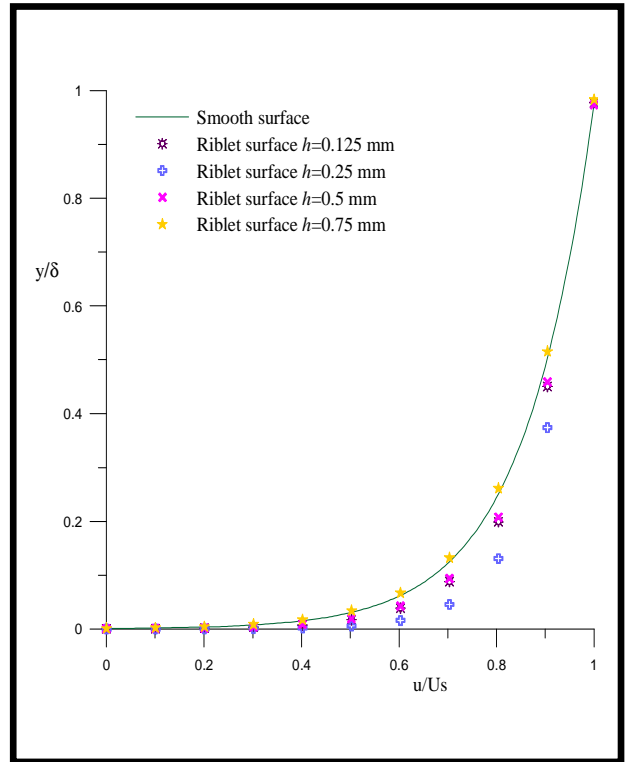


(b) Straight riblet with $w=2, h=0.25\text{mm}$

Figure 6. Velocity profile through the boundary layer at $x=0.51L$.

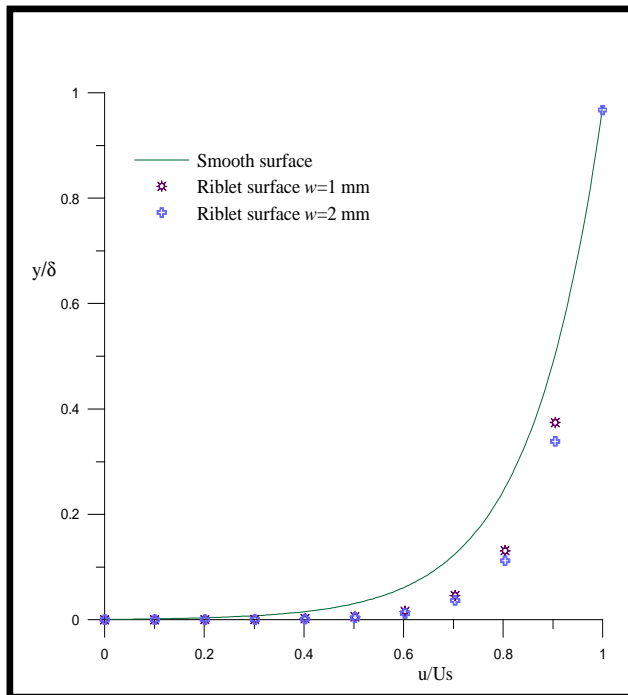


(a) Straight riblet with $s=2, h=0.25\text{mm}$

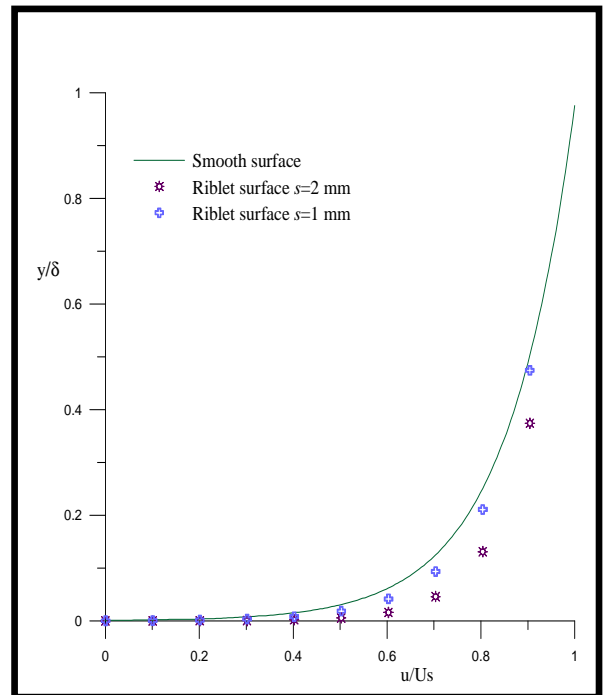


(b) Sinusoidal riblet with $w=1, s=2\text{mm}$

Figure 7. Velocity profile through the boundary layer at $x=0.51L$.

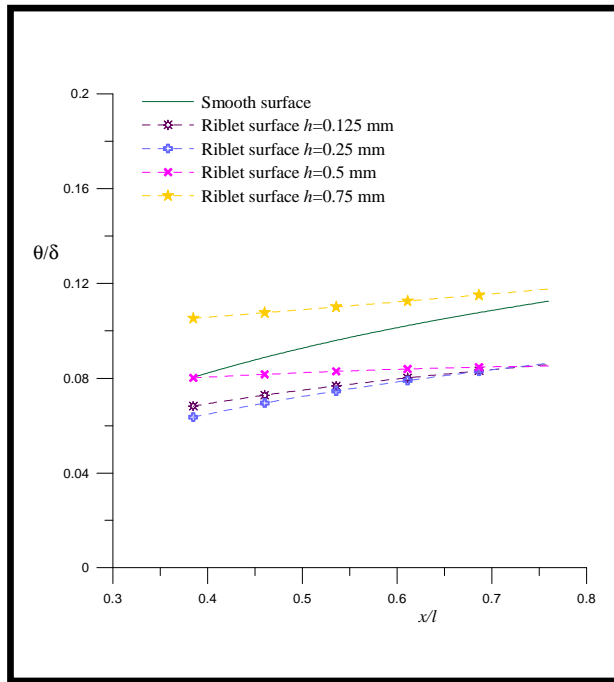


(a) Sinusoidal riblet with $s=2, h=0.125\text{mm}$

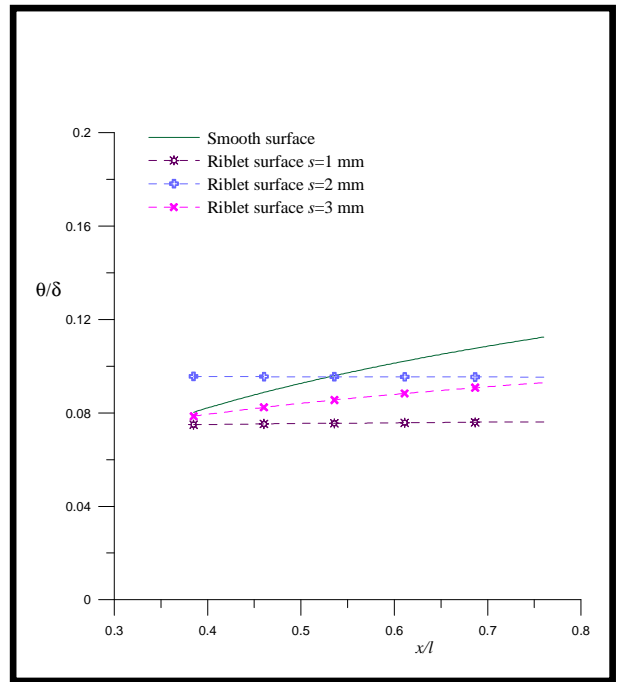


(b) Sinusoidal riblet with $w=1, h=0.125\text{mm}$

Figure 8. Velocity profile through the boundary layer at $x=0.51L$.

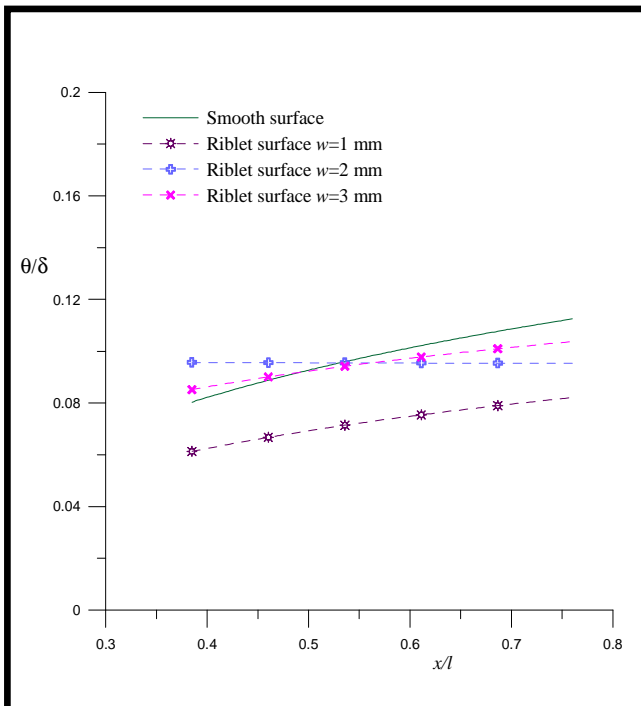


(a) Straight riblet with $w(=s)=1\text{mm}$

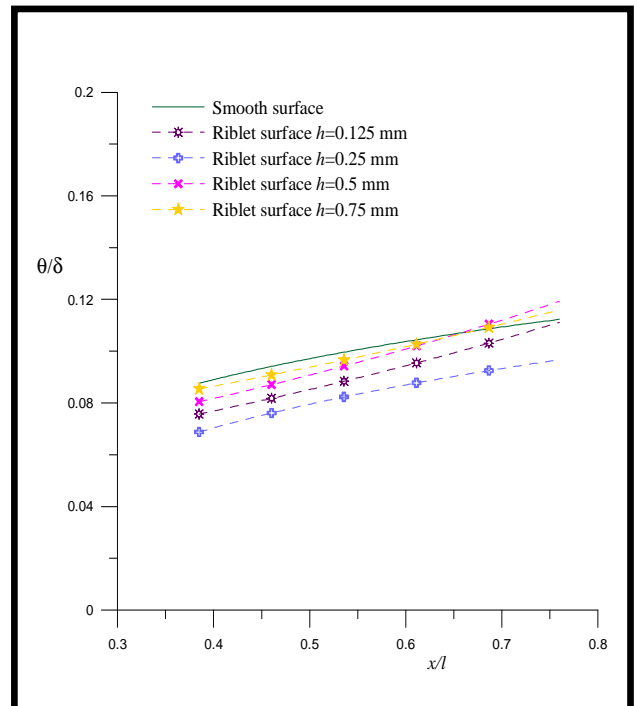


(b) Straight riblet with $w=2, h=0.25\text{mm}$

Figure 9. Riblet effect on the momentum thickness.

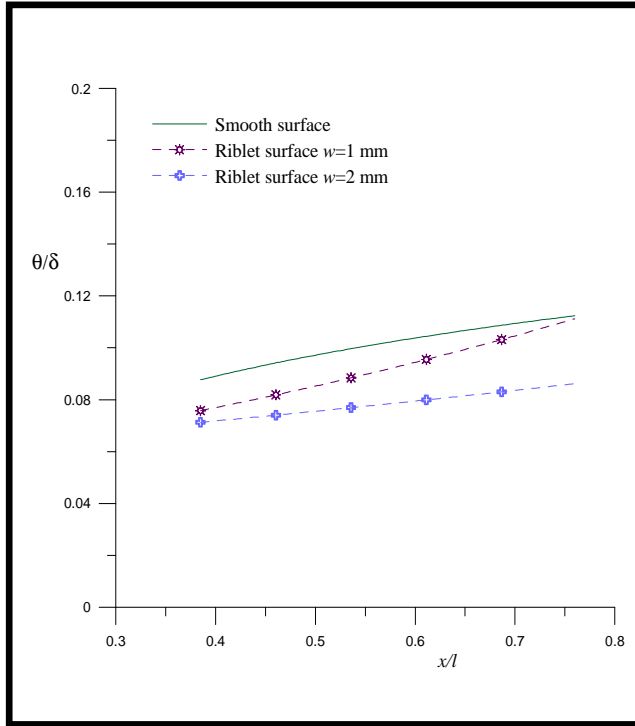


(a) Straight riblet with $s=2, h=0.25\text{mm}$

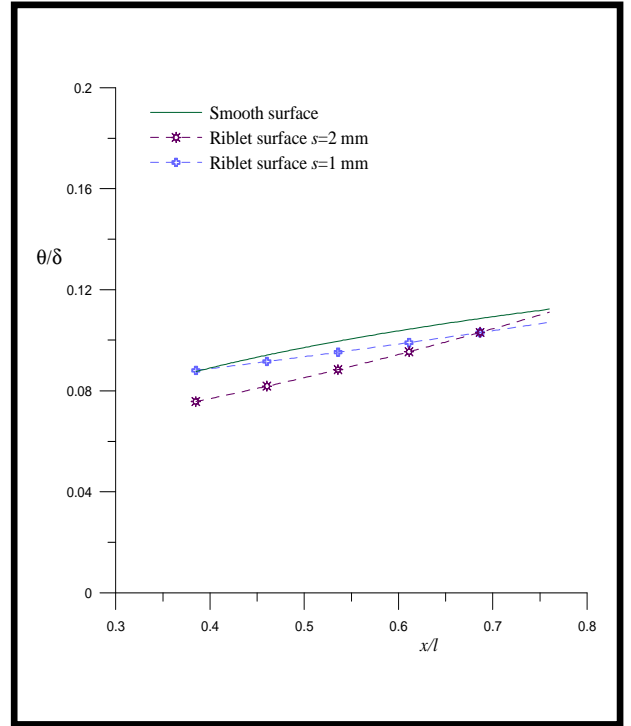


(b) Sinusoidal riblet with $w=1, s=2\text{mm}$

Figure 10. Riblet effect on the momentum thickness.

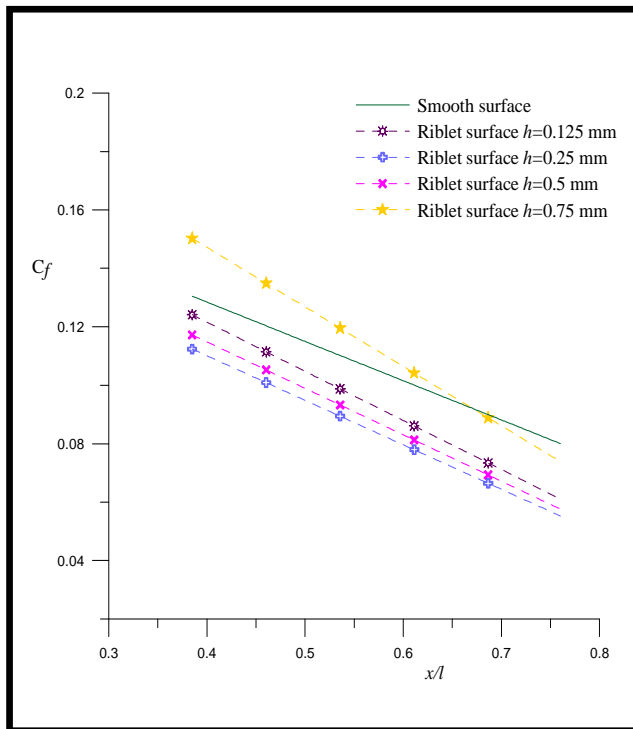


(a) Sinusoidal Riblet with $s=2, h=0.125\text{mm}$

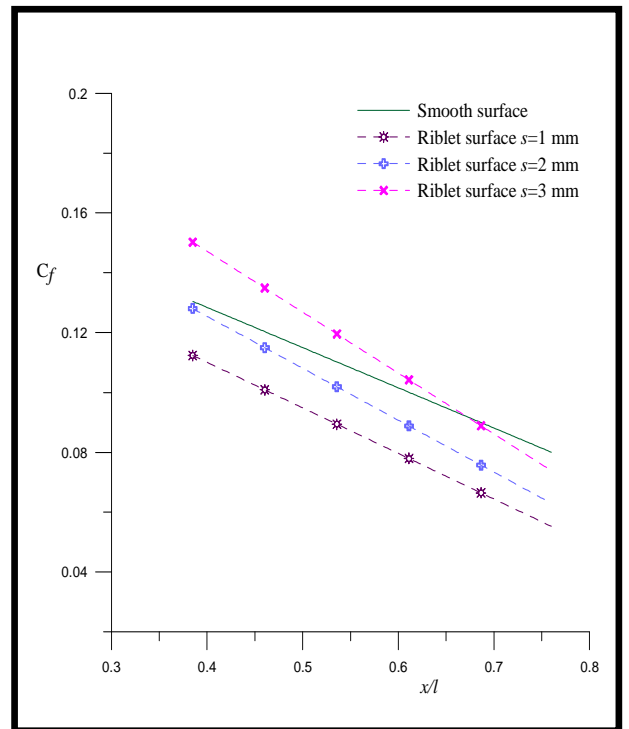


(b) Sinusoidal Riblet with $w=1, h=0.125\text{mm}$

Figure 11. Riblet effect on the momentum thickness.

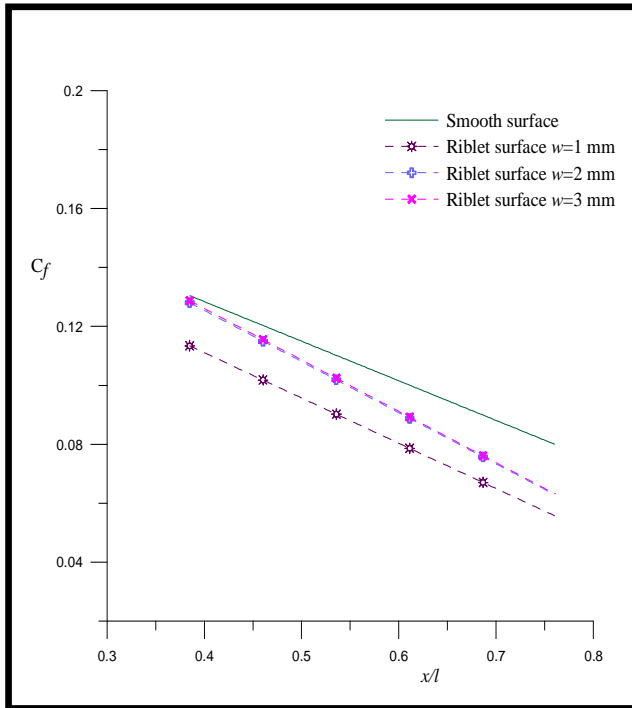


(a) Straight riblet with $w(=s)=1\text{mm}$

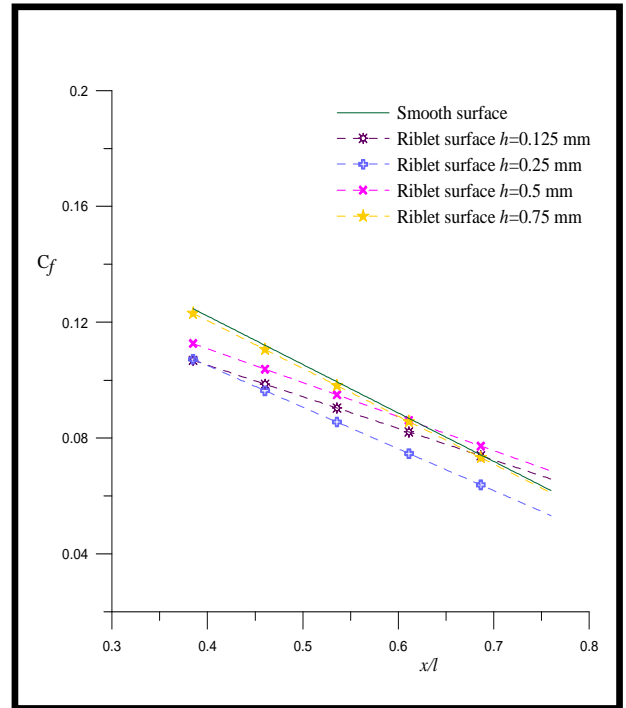


(b) Straight riblet with $w=2, h=0.25\text{mm}$

Figure 12. Skin friction coefficient distribution along the plate.

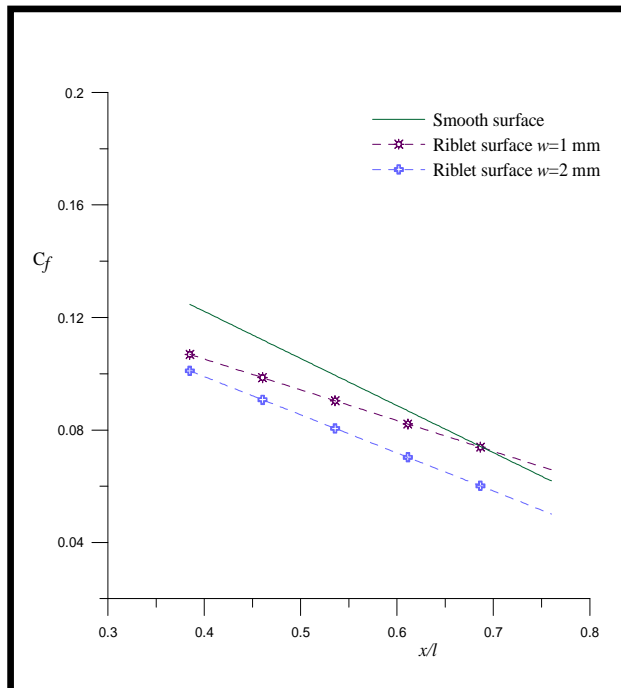


(a) Straight riblet with $s=2, h=0.25\text{mm}$

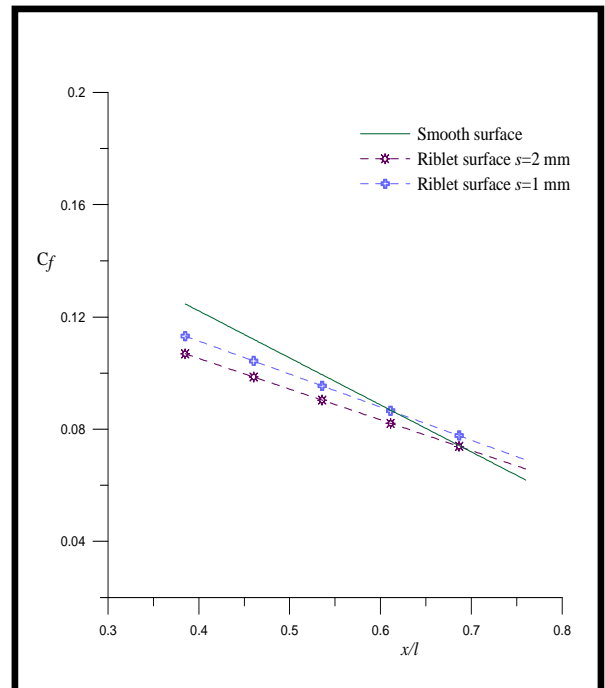


(b) Sinusoidal riblet with $w=1, s=2\text{mm}$

Figure 13. Skin friction coefficient distribution along the plate.

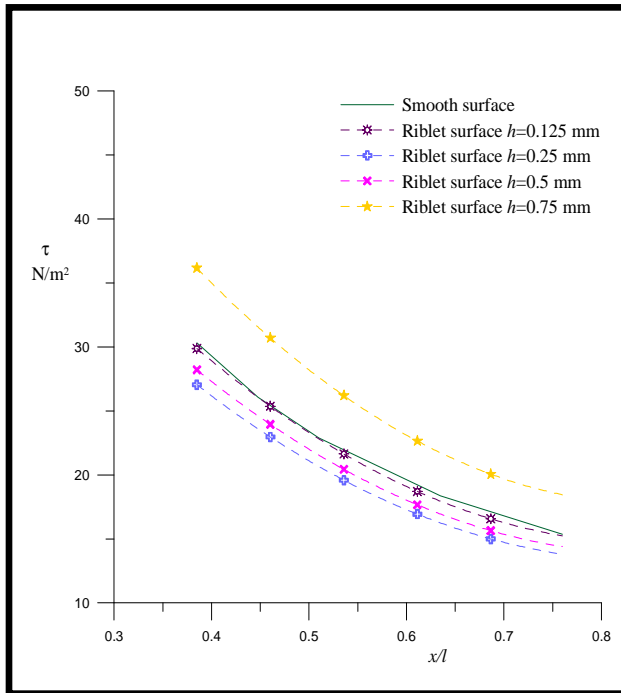


(a) Sinusoidal riblet with $s=2, h=0.125\text{mm}$

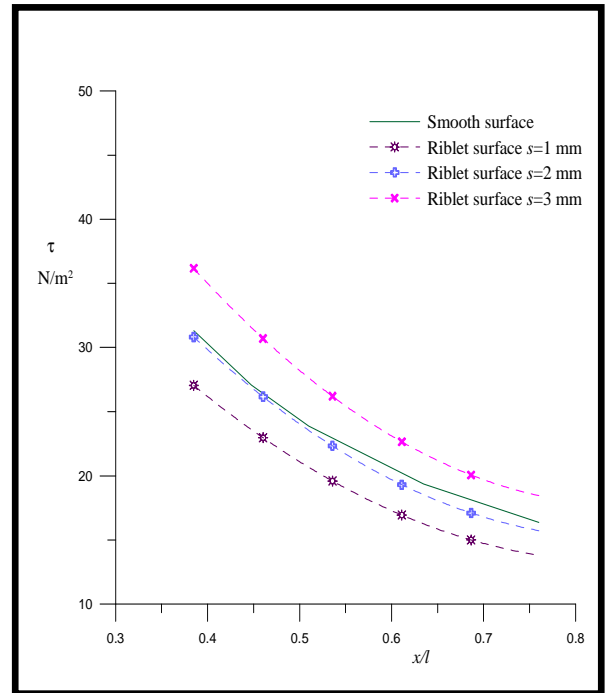


(b) Sinusoidal riblet with $w=1, h=0.125\text{mm}$

Figure 14. Skin friction coefficient distribution along the plate.

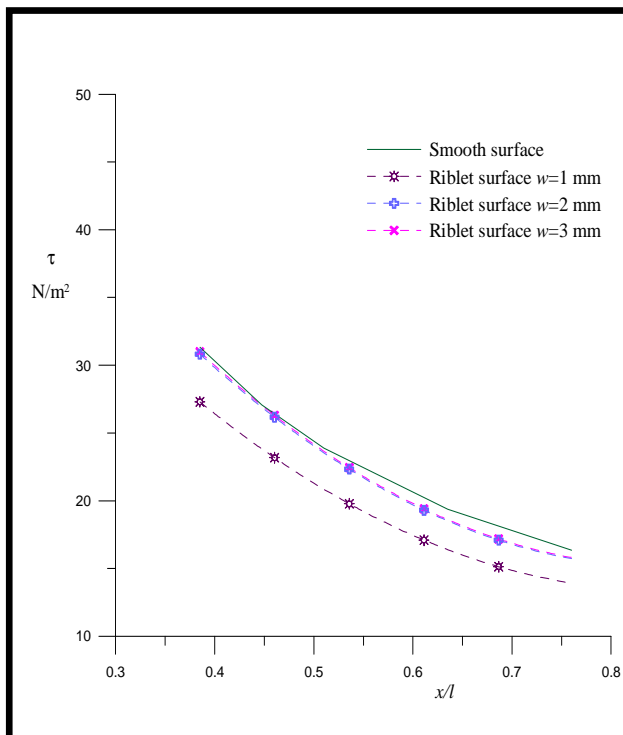


(a) Straight riblet with $w(=s)=1\text{mm}$

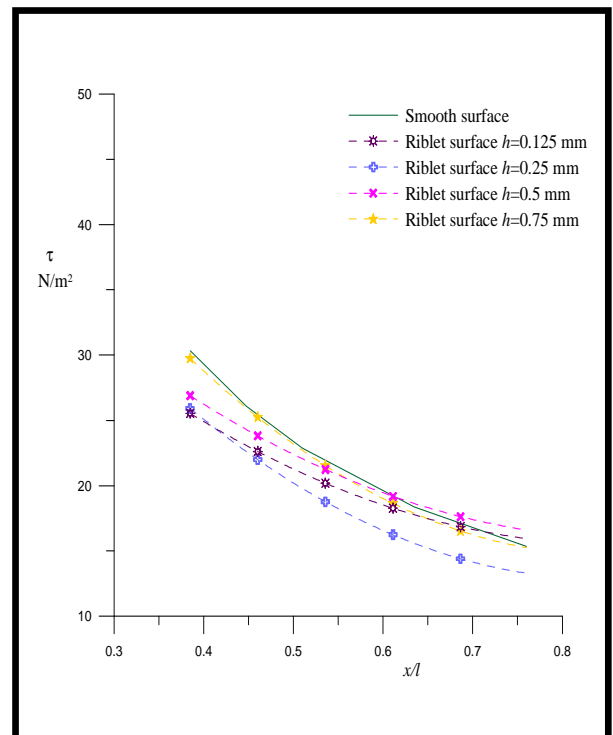


(b) Straight riblet with $w=2, h=0.25\text{mm}$

Figure 15. Wall shear stress distribution along the plate.

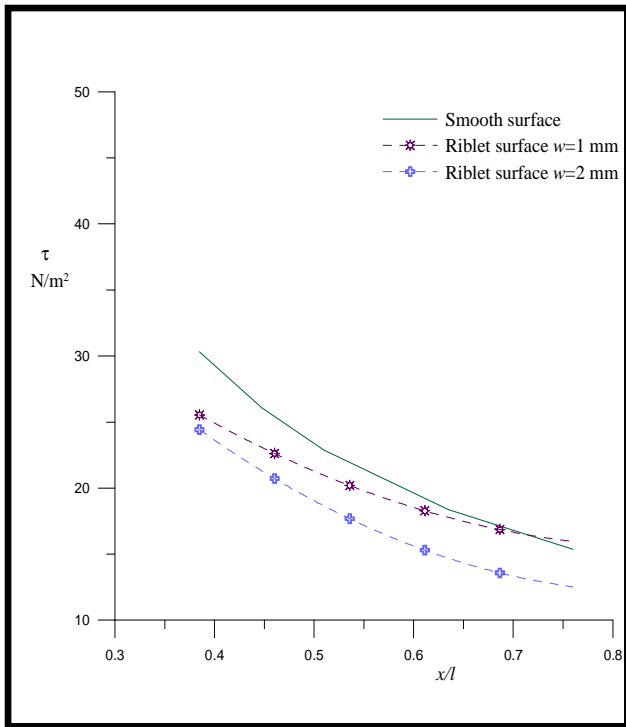


(a) Straight riblet with $s=2, h=0.25\text{mm}$

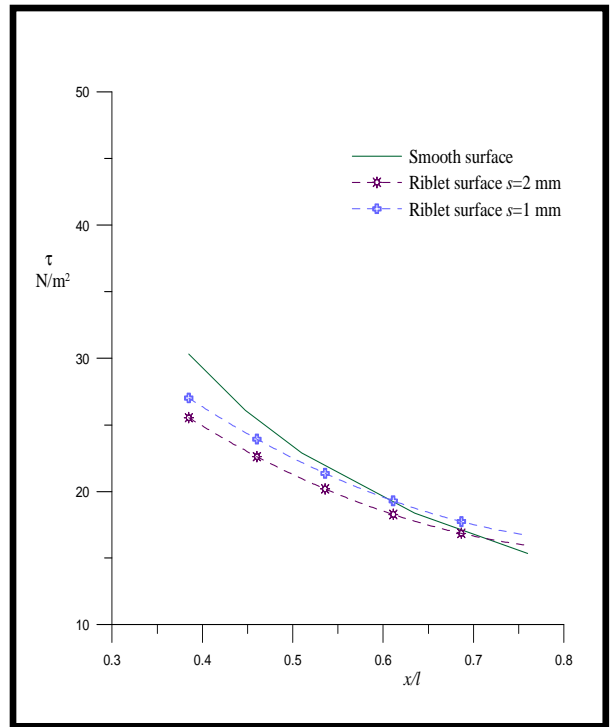


(b) Sinusoidal riblet with $w=1, s=2\text{mm}$

Figure 16. Wall shear stress distribution along the plate.

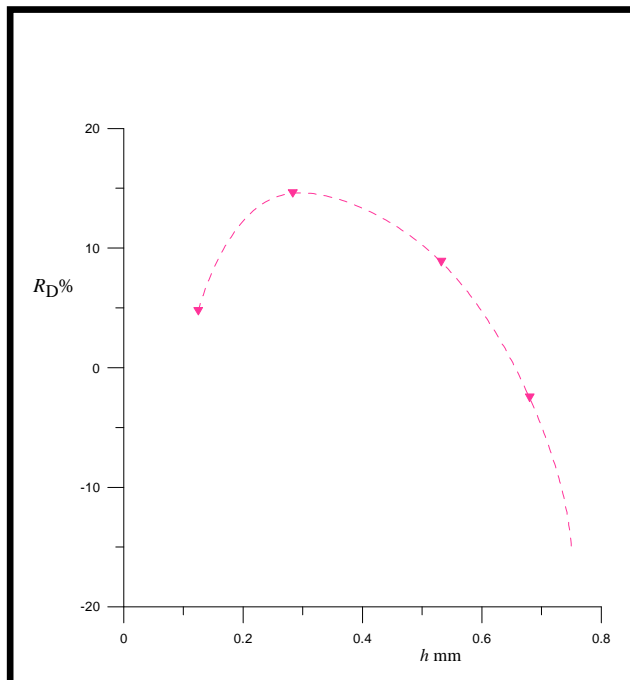


(a) Sinusoidal riblet with $s=2, h=0.125\text{mm}$

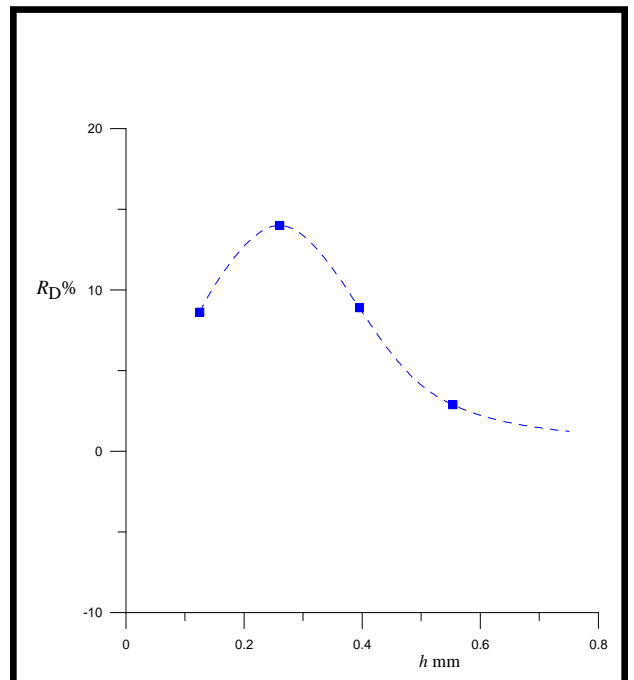


(b) Sinusoidal riblet with $w=1, h=0.125\text{mm}$

Figure 17. Wall shear stress distribution along the plate.



(a) Straight riblet with $w(=s)=1\text{mm}$



(b) Sinusoidal riblet with $w=1, s=2\text{mm}$

Figure 18. Effect of riblet height on the drag reduction.

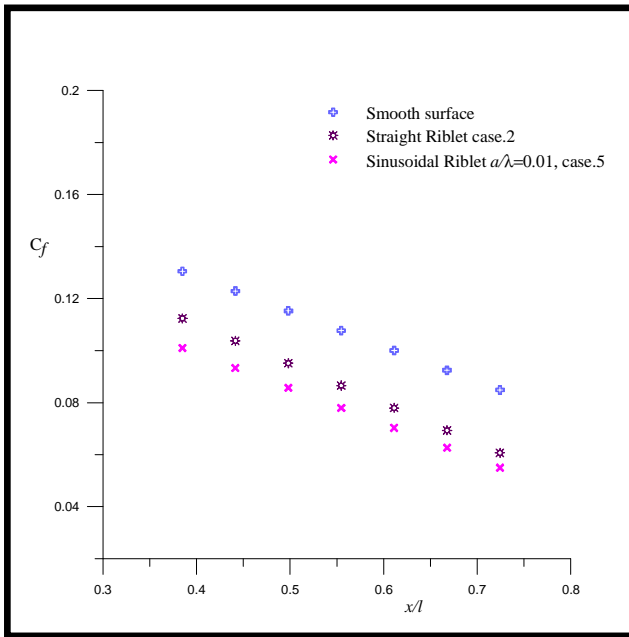


Figure 19. Skin friction coefficient comparison at $Re=4.9 \times 10^5$.

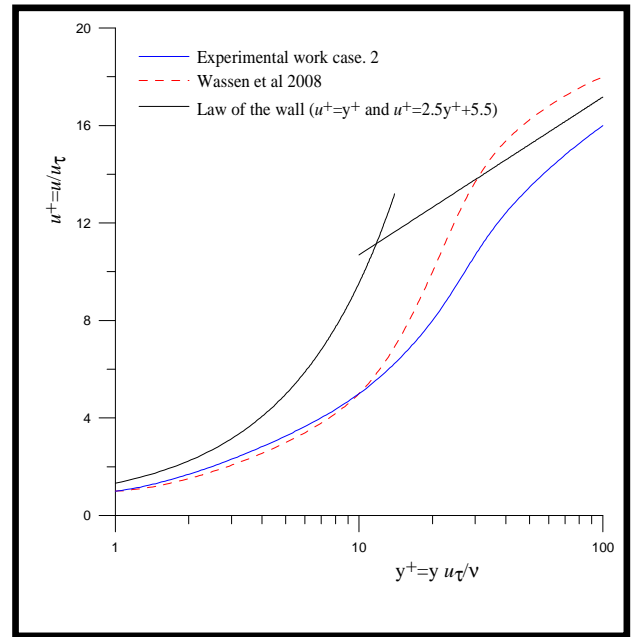


Figure 20. Mean velocity profiles comparison for straight riblet, v : kinematic viscosity.

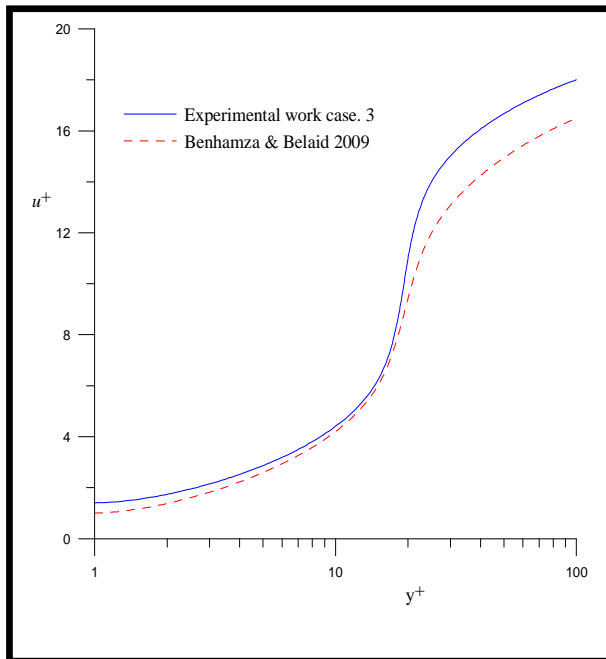


Figure 21. Mean velocity profiles comparison for straight riblet.

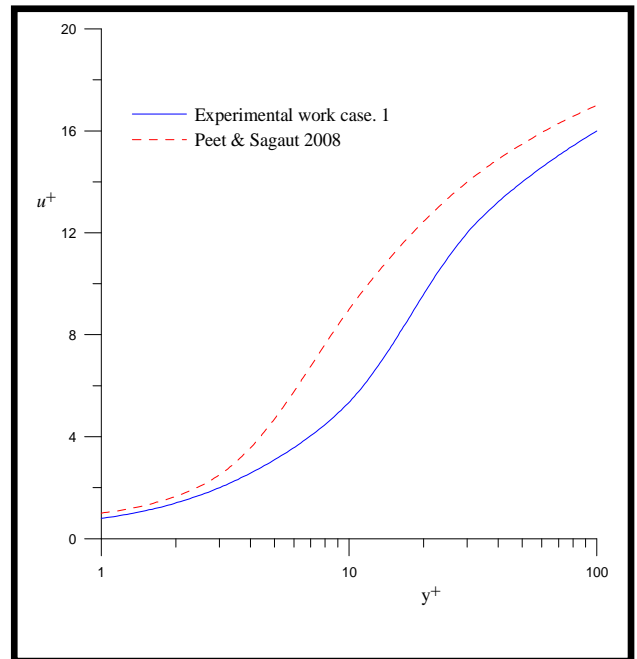


Figure 22. Mean velocity profiles comparison for sinusoidal riblet.